Evaluating targeted combination therapies in EGFR wild-type non-small-cell lung cancer using mass spectrometry-based proteomics

Master Thesis at the Department of Immunotechnology (LTH) in affiliation with Karolinska Institutet

Johan Thorsson

Supervisor: Prof. Dr. Sara Ek

Deputy supervisors: Assoc Prof. Dr. Lukas Orre,

Olena Berkovska (MSc in Pharmaceutical Science) and Dr. Yanbo Pan

Examinator: Assoc Prof. Dr. Fredrik Levander

Duration: 29-08-2022 – 08-02-2023

Abstract

Survival for non-small cell lung cancer (NSCLC) patients has been significantly improved by epidermal growth factor receptor (EGFR) tyrosine kinase inhibitors (TKIs) in patients with EGFR mutations. However, certain subpopulations of NSCLC patients with EGFR wild-type (wt) status have been shown to also respond to EGFR-TKIs. In an effort to stratify EGFRwt tumors, our group discovered in previous experiments that CDKN2A deletion could be used as a predictive biomarker for EGFR-TKI response. In this setting, we also discovered synergism between EGFR-TKIs and inhibition of the anti-apoptotic protein Bcl-xl. Evaluation of this combination treatment in a lung cancer EGFRwt cell line with CDKN2A deletion, NCI-H292, revealed that an early adaptation upregulation of cholesterol synthesis could be a possible resistance mechanism. Thereby, we hypothesized that the effectiveness of this combination treatment could be further improved by the addition of cholesterol synthesis inhibitors, *i.e.*, statins. In the present project, we investigated the triple-drug combination of afatinib, A-1331852 and simvastatin *in vitro*, and the results displayed a reduced NCI-H292 viability compared to two-drug combinations or monotherapies of the three drugs. Then, by performing in-depth mass spectrometry (MS)-based molecular profiling we were able to detect patterns linked to primary resistance mechanisms of statin treatments such as feedback upregulation of the drug target 3-hydroxy3-methylglutaryl coenzyme A reductase (HMGCR). Patterns related to successful treatment such as cell cycle arrest were also detected. Taken together, these results indicate that the suggested triple combination could be used with lower concentrations of drugs involved and thereby possibly reduce unwanted side effects while at the same time being more effective.

Introduction

Cancer is one of the leading causes of death in the world, thereby causing suffering and a large socioeconomic burden. With 2.21 million new cases each year, lung cancer is the second most common type of cancer [1]. With early detection and diagnosis of cancer, therapies can be curative. However, 47% of lung cancer cases are detected at a late stage of the disease, when the primary tumor has metastasized (stage IV) [2]. Since surgery and radiotherapy are no longer an option at this stage, systemic therapies such as chemotherapy, targeted therapies, or immunotherapies are used to achieve prolonged survival [3]. Lung cancer can histologically be divided into small cell lung cancer (SCLC) and non-small cell lung cancer (NSCLC), with a 5-year survival rate of 7% for late-stage NSCLC patients [4]. Further, NSCLC is currently subtyped based on histology and the presence of biomarkers such as immune checkpoint proteins [5, 6]. Due to the large heterogeneity of the disease and frequently observed drug resistance, patient stratification is indisputably needed. To tailor patient-specific treatments, an understanding of tumor biology, diagnostic-, predictive- and prognostic biomarkers as well as druggable targets are essential [6]. In line with this, targeted therapies could be used with the benefit of having fewer unwanted side effects compared to chemotherapy [7].

Targeted therapies have been successful in prolonging survival in subsets of NSCLC patients [8]. Eventually, relapse follows in most cases due to drug resistance [8]. By defects in DNA repair causing genomic instability, rapid evolution can take place with a selection pressure favoring cell clones that are less sensitive to treatment. Thereby, resistance to a drug can be acquired by, *e.g.*, on-target mutations making the drug unable to bind to the target proteins [8]. Off-target resistance, on the other hand, is acquired by the regulation of other proteins either downstream of the drug target or in alternative pathways bypassing the targeted pathway [8]. The oncogenic signaling of NSCLC has a high plasticity and therefore involved cells have more potential to adapt to changes in the microenvironment (*e.g.*, presence of a drug molecule) through rewired signaling. This form of resistance is related to lack of treatment response due to its immediate activation. Altered regulation like this has been shown to be rapidly induced as a response to targeted therapies in NSCLC [9]. Many types of treatment-induced resistance mechanisms have previously been explained; therapy-induced senescence (TIS) being one of them. During exposure to sub-toxic levels of drugs, cells can enter an anti-proliferative state and thereby persist indefinitely with comprised viability while still contributing to tumor progression through oncogenic signaling. Additionally, drug-induced trans-differentiation such as epithelial-to-mesenchymal transition (EMT) has been explained as a resistance mechanism where epithelial cells acquire a motile mesenchymal phenotype [10].

The most commonly used targeted therapy in NSCLC targets epithelial growth factor receptor (EGFR). EGFR is inhibited by antibodies or tyrosine kinase inhibitors (TKIs). Clinical trials revealed that patients with activating mutations on EGFR show better responses to EGFR-TKIs compared to standard chemotherapy [11]. However, in 40–80% of NSCLC cases, EGFR is shown to be overexpressed, indicating that inhibition of the receptor could have an effect even in NSCLC patients with wild-type (wt) EGFR [12]. Furthermore, when EGFR-TKIs were compared to docetaxel as second-line therapy in NSCLC patients with EGFRwt, the best responses were found in the docetaxel patient group. Nevertheless, stable disease was obtained in some of the patients on EGFR-TKIs therapy, indicating anticancer effects in a subgroup of patients with EGFRwt lung cancer [13].

To investigate determinants of EGFR-TKI response in EGFRwt lung cancer, Orre et al. analyzed public domain data, revealing that in EGFRwt NSCLC cell lines, epithelial cell lines

were more sensitive to EGFR-TKIs than mesenchymal cell lines (unpublished data). Furthermore, the group used identified EGFRwt epithelial cell lines with EGFRmutant-like molecular response to EGFR-TKI treatment. Interestingly, the tumor suppressor CDKN2A was found deleted in most of the mutant-like responding cells, and therefore it was hypothesized to be a biomarker for treatment response prediction. To continue, the monotherapy indicated an intermediate response to EGFR-TKI and therefore increased efficiency was hypothesized to be reached by combination therapy. To investigate this further, a high-throughput screening (HTS) analysis of 528 targeted therapies in combination with gefitinib was performed to find candidates for combination treatment together with EGFR-TKI. In this screen, Bcl-xL (B-cell lymphoma-extra large) inhibitors (Bcl-xLi) were found to have synergistic effects together with EGFR-TKIs and were therefore selected to be evaluated for a new combination therapy. Interestingly, Bcl-xL has previously been associated with resistance to targeted therapies [14], and in support of this finding, two of the EGFR mutant-like responding cell lines in the investigated panel had high protein levels of Bcl-xL. A new MS-based molecular profiling was performed to evaluate the combination of EGFR-TKI and Bcl-xLi. By doing so, senescence was pointed out to be a possible treatment escape mechanism to EGFR-TKI since the monotherapy displayed activation of senescence inducers CDKN1A and CDKN1B [15]. The addition of Bcl-xLi led to decreasing levels of both these inducers, thereby it was acting as a senolytic compound which could explain the combination effect of these two drugs.

Subsequent MS-based molecular response profiling of EGFR-TKI/Bcl-xLi combination therapy revealed an increase in proteins involved in cholesterol synthesis in response to the new treatment. Cholesterol is synthesized via the mevalonate pathway which is known to have aberrant regulation in many cancers [16, 17]. The mevalonate pathway can be therapeutically targeted with statins, a group of inhibitors that competitively bind to the active site of 3-hydroxy3-methylglutaryl coenzyme A reductase (HMGCR) which is the rate-limiting enzyme of the mevalonate pathway [18]. Since statins were approved already in 1987 by U.S. food and drug administration (FDA) for treating hypercholesterolemia, the toxicity patterns are well documented [19, 20]. By blocking HMGCR, statins trigger feedback transcriptional activity of sterol regulatory element-binding protein (SREBP) which causes upregulation of HMGCR and low-density lipoprotein (LDL) receptor. These receptors are responsible for the exogenous uptake of LDL [21]. Interestingly, statins have shown promising results as anti-cancer agents through multiple mechanisms, a subset of these mechanisms rely on geranylgeranyl pyrophosphate (GGPP) which is a downstream product of the mevalonate pathway [22]. Depletion of GGPP has shown anti-cancer effects through lowered nutrient uptake by micropinocytosis [23], less prenylation of oncoproteins such as RAS and RHO [24] and lower levels of coenzyme Q (CoQ) [25, 26]. Therefore, the repurposing of statins for cancer treatment has gained a lot of interest lately. In a Phase II clinical trial simvastatin, a lipophilic type of statin improved tumor response rates and progression-free survival (PFS) when combined with the EGFR-TKI gefitinib compared to gefitinib alone in EGFR wild-type nonadenocarcinomas[27]. Furthermore, retrospective studies of three clinical trials in blood cancers revealed enhanced efficacy of venetoclax (Bcl-2 inhibitor) for patients who were concurrently on statin treatment [28].

Based on these findings, we hypothesized that altered metabolism could limit the effect of EGFR-TKI (afatinib) /Bcl-xLi (A-1331852) combination treatment. so thereby we wanted to test if the addition of simvastatin could further increase the efficiency of the combination treatment. Here in we performed drug sensitivity and resistance testing (DSRT) as well as mass MS-based protein-level molecular profiling to test the effectiveness of such a triple combination therapy. DSRT revealed that the triple combination showed greater efficacy compared to

afatinib and A-1331852 combination. With in-depth molecular profiling, we were able to identify 9903 proteins. Further on with differential expression analysis and gene set enrichment analysis, we were able to detect patterns both linked to effective statin treatment and primary resistance mechanisms.

Materials and Methods

Cell culture and drug treatment for drug screening and proteomics analysis

NCI-H292 (ATCC, Manassas, VA, USA) cells were expanded and cultured in RPMI 1640 medium (R2405, Sigma-Aldrich, St. Louis, Missouri) with 10% fetal bovine serum (FBS, F7524, Sigma-Aldrich) and 1% penicillin-streptomycin (P4333, Sigma-Aldrich) at 37 °C, 5% CO_2 and 90% humidity. Drug screening was prepared with all three drugs being dispensed into 384-well plates (CLS-3764, Sigma-Aldrich) for drug sensitivity and resistance testing (DSRT) by using a Labcyte Echo 550 (Labcyte Inc.). The following concentrations were used; afatinib (S7801, Selleckchem) 0–1500 nM (10 measurements points, 10-fold dilution), A-1331852 (S1011, Selleckchem) 0–3333 nM (8 measurement points, 10-fold dilution) and simvastatin (154-10010344-5, Selleckchem) 0–1000 nM (8 measurements points, 10-fold dilution). Cells treated with dimethyl sulfoxide (DMSO) were used as negative controls. Biological triplicates were used for every possible combination, except for afatinib 1500 nM which was only tested as a singlet. MultiDrop Reagent Dispenser with a Standard tube dispensing cassette (24072670, Thermo) was used for seeding 1800 NCI-H292 cells per well. After a 72-h incubation, viability testing was performed using CellTiter-glo (CTG) assay (G9241, Promega), luminescence was consequently measured using Perkin Elmer EnSight Plate Reader. Viability was calculated according to **Equation 1** where the negative control is DMSO alone and the positive control is 100 μM benzethonium chloride. Drug treatment for proteomic analysis was performed by seeding 2 million cells onto 10-cm dishes. After a 18-h incubation, treatment was initiated by switching to fresh medium with 1.5 mM afatinib, 1 mM A-1331852 and 1 mM simvastatin in combinations (see also **Figure 2A**). After 24 h of treatment, cells were harvested and washed with phosphate buffered saline PBS (14190-144, Gibco, United Kingdom) and trypsinized with TrypLE (12604-021, Gibco, Denmark) and harvested with the assistance of a cell scraper.

$$100 - 100(\overline{Ctrl}_{Neg} - well\ signal)/(\overline{Ctrl}_{Neg} - \overline{Ctrl}_{Pos})$$

Equation 1. Calculation of cell viability.

Sample preparation for proteomic analysis

Cell lysis was performed by adding lysis buffer (4% (w/v) sodium dodecyl sulfate (SDS)(Fluka), 25 mM HEPES pH 7.6 (Sigma Aldrich), 1 mM dithiothreitol (DTT) (Sigma)) to pelleted cells. Samples were then heated for 5 min at 95 °C and disrupted by sonication (Am 50%, 60 s, pulse 1.0 s). Protein concentration was then determined using DC protein assay kit (5000112, BioRad). Protein lysate (150 μg of protein) from each sample was diluted with lysis buffer and then protein cleanup was done according to single-pot, solid-phase-enhanced, sample-separation (SP3) protocol [29]. Proteins were then digested by sequential addition of lysC endopeptidase (129-02541, Lys-C, Wako, Neuss, Germany) and trypsin (Thermo Fisher Scientific). First digestion was performed with lysC at 37 °C for 4 h with an Enzyme/protein ratio of 1:50 diluted in 50 mM HEPES pH 7.6 and 1 M urea. This was followed by an additional 14-h digestion with trypsin diluted in 50 mM HEPES pH 7.6 at the same temperature and with the same enzyme/protein ratio. Peptide concentration measurement was performed on the peptide solution with BioRad DC Protein Assay kit and a correction factor of 0.8 was applied

to absorbance values for calculating peptide quantities. Peptides from each sample (50 µg) were then labeled with tandem mass tag TMT-18plex (A52045, Thermo Scientific) isobaric label according to the manufacturer's instruction. Samples were then pooled and cleaned with Strata-X-C-cartridge (Phenomenex, Torraence, California) and then dried in a vacuum centrifuge (Electron Savant Speedvac, Thermo Fisher Scientific).

Peptide prefractionation with high-resolution isoelectric focusing (HiRIEF)

TMT labeled peptides were separated based on isoelectric point as previously explained by Branca et al. [30] using two custom-made 24-cm long IPG (immobilized pH gradient) gel strips provided by GE Healthcare Bio-Sciences, one narrow range pH 3.7-4.9 and one broad range pH 3-10. The narrow range strip was re-swelled overnight with a rehydration solution containing 8 M Urea, Bromophenol blue and 1% Pharmalyte, pH 2.5-5 (GE Healthcare). In parallel, 300 µg of labeled peptides was dissolved in 8 M Urea with Bromophenol blue and then used for re-swelling a gel bridge overnight. The broad range strip was re-swelled overnight with 300µg of TMT labeled peptides dissolved in 8M Urea, bromophenol blue and Pharmalyte, pH 3-10 (GE Healthcare). Iso-electric focusing was then performed using an Ettan IPGphor (GE Healthcare) and for the narrow range strip, the gel bridge was placed on top of the IPG strip at the cathode end. The narrow range strip was in the machine until 347 kV-h was reached and the narrow broad strip until 153 kV-h was reached. After focusing a liquid handling robot Etan digester from GE Healthcare Bio-Sciences AB, which is a modified Gilson liquid handler 215) was used to extract the peptides from the strips. A polypropylene well former was put on gel strips forming 72 wells. Then 30 minutes of incubations were done with first MQ water, then 35 % acetonitrile followed by 35% acetonitrile with 0.1% formic acid. After every incubation liquid was transferred into a 96-well plate. Then samples were dried in a vacuum centrifuge.

Relative quantitation with LC-MS

LC-MS was performed on the two 96-well plates in sequence. For every HiRIEF fraction an autosampler (Ultimate 3000 RSLC system, Thermo Scientific Dionex) mixed mobile phase A (95% water, 5% DMSO 0.1% formic acid) with dried peptides. Fractions were dissolved and fractions from the broad range strip were combined to a total of 40 wells. Fractions were then injected into a C18 trap desalting column (Acclaim pepmap, C18, 3 µm bead size, 100 Å, 75 µm × 20 mm, nanoViper, Thermo). The loading pump was used for 5 minutes and then analysis mode was engaged by switching to NC pump. A curve gradient with phase B (90% acetonitrile, 5% DMSO, 5% water, 0.1% formic acid) was applied (curve 6 in the Chromeleon software). Then a nano EASY-Spray column (pepmap RSLC, C18, 2 µm bead size, 100Å, 75 µm × 20 mm, Thermo) was used on the nano electrospray ionization (NSI) EASY-spray source (Thermo). A hybrid Q-Exactive HF mass spectrometer (Thermo scientific) was used for online LC-MS. FTMS master scans were used with a mass range of 300-1500 *m/z*, then data-dependent MS/MS was performed on the top 5 precursor ions which were selected for fragmentation by high-energy collision dissociation (HCD). Precursor isolation was done with a window of 2 *m/z*. Maximum injection time was set to 100ms for both MS1 and MS2 and a duty cycle lasted roughly 1 s. precursors having a charge state of 2-7 were included. Peptide and protein identification was performed with Proteome Discoverer (v2.4), MSF files were used as input with the protein database Homo sapiens (sp_incl_isoforms TaxID=9606) (v2022-10-12) and

for dynamic modifications, oxidation was allowed, and for static modifications, n terminus TMT pro and C-Terminus TMT-pro and Carbamidomethyl was applied.

Bioinformatic analysis

In downstream bioinformatic workflow, BREEZE[31] was used for quality control of drug screening, R version (4.1.0) was used to analyze proteomics data. Identified proteins were filtered based on a false discovery rate (FDR) of 1 %. Relative abundance was calculated by dividing all samples with the mean of control samples (n=3) and then further normalized and log2 transformed. Principal-component analysis was performed with prcomp [32] function and for hierarchal clustering, ComplexHeatmap (version 2.10.0) [33] was used. Furthermore, DEqMS version (1.16.0) [34] was used for statistical analysis of protein differential expression, and for gene set enrichment analysis ClusterProfiler (version 4.2.2) [35] was used.

Results

Drug screening indicates combination-therapy dependent effects on the viability of CDKN2A deleted EGFRwt epithelial lung cancer cells

To evaluate treatment response and potential synergy in combination therapies, a CDKN2A deleted epithelial lung cancer cell line (NCI-H292) was subjected to high-throughput drug sensitivity and resistance testing (DSRT) with simvastatin, afatinib (EGFR-TKI) and A-1331852 (Bcl-xLi) as outlined in **Figure 1a**. The DSRT analysis supported the hypothesis that the addition of simvastatin could potentiate the effect of EGFR-TKI/Bcl-xLi combination therapy, specifically for higher concentrations of afatinib and A-1331852 (**Figure 1b-c**). Furthermore, neither simvastatin monotherapy nor A-1331852 monotherapy did reach a cell viability below 70% (**Figure 1d**). Reproduced results could be obtained from prior experiments performed in the group as a significant decrease in viability was obtained in this experiment when comparing afatinib monotherapy with afatinb combined with A-1331852 for afatinib 0.23 (nM). Otherwise afatinib and A-1331852 combination displayed similar response in viability as afatinib monotherapy. The addition of simvastatin alone, at fixed concentrations 333 nM failed to substantially improve afatinib response, with 40% viability as the maximum effect reached at the highest afatinib concentration used (**Figure 1d**). However, the triple combination (afatinib with A-1331852 fixed at 123 nM and simvastatin at 333 nM) resulted in improved effect with around 20% cell viability at the highest afatinib concentration (**Figure 1d**).

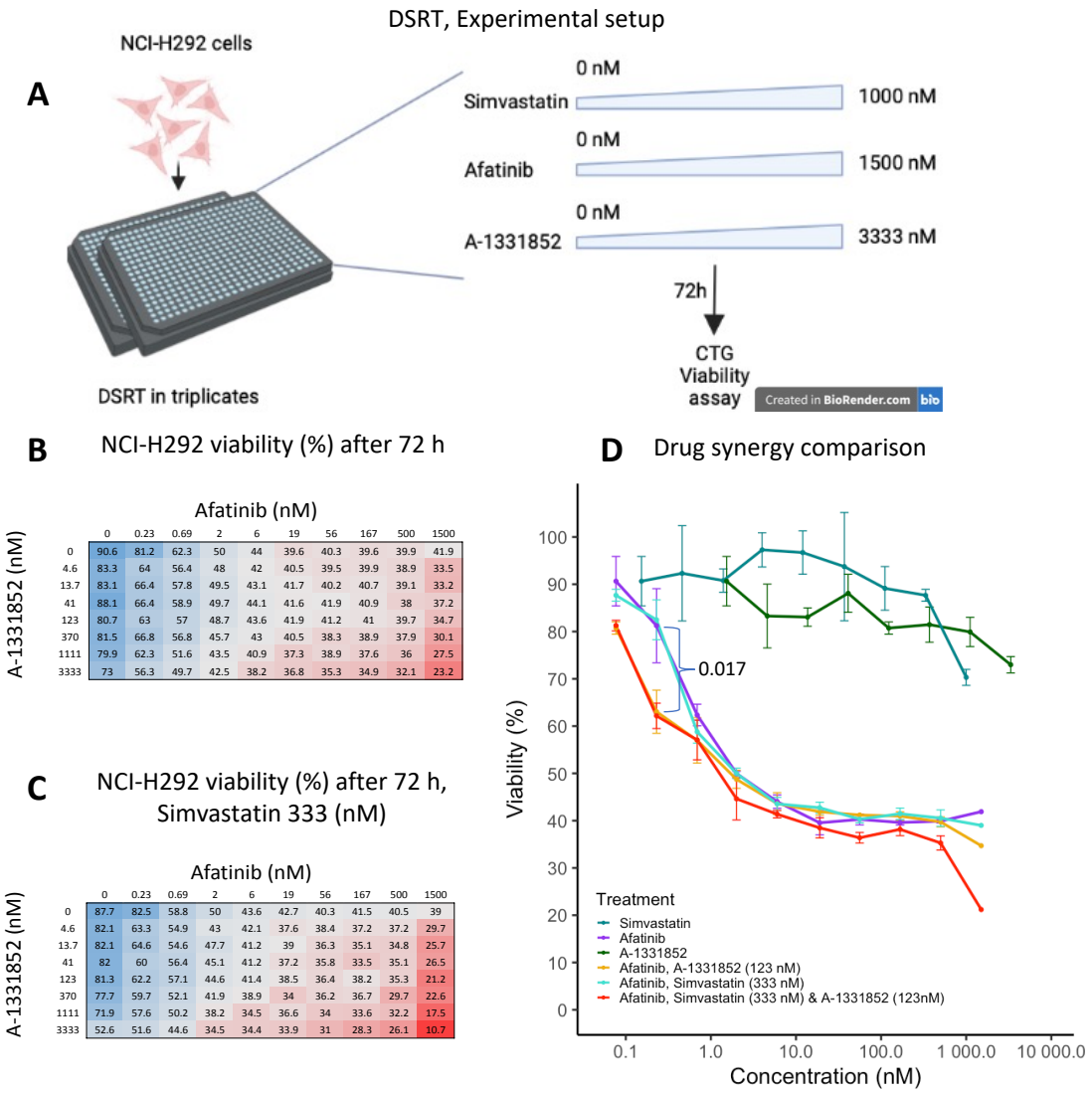

Figure 1. Synergistic effects can be observed in afatinib, A-1331852 & simvastatin combination treatment using drug sensitivity testing. **A**. The experimental setup for triple combination drug sensitivity testing (DSRT). Briefly, cells were seeded in triplicates in 384-well plates containing all possible concentration combinations of afatinib, A-1331852 and simvastatin, ranging from 0 to 1500, 3333, and 1000 nM, respectively. After a 72-hour incubation, viability was measured with a CTG assay. **B**. DSRT results for the double combination of afatinib and A-1331852 in different concentrations, represented as the mean cell viability (n = 3 cell culture wells, except n = 1 for the treatments with 1500 nM afatinib). **C**. DSRT results for triple combination of simvastatin (333 nM) with afatinib and A-1331852 (range of concentrations), represented as the mean cell viability (n = 3 cell culture wells, except n = 1 for the treatments with 1500 nM afatinib). **D**. Drug response to different combinations across a range of afatinib concentrations, represented as mean viability ± standard deviation (n = 3 cell culture wells, except n = 1 for the treatments with 1500 nM afatinib). P-value indicated between afatinib 0.23 (nM) and afatinib 0.23 (nM) with A-1331852 123 (nM).

Molecular profiling of NSCLC cells after treatment

MS-based molecular response profiling after treatment with simvastatin, afatinib or A-1331852 of epithelial cancer cell line (NCI-H292) was performed as outlined in **Figure 2A**. In total, 9903 proteins (gene-centric analysis) were identified and quantified in the 15 samples. Principal component analysis (PCA) (**Figure 2B)** and unsupervised clustering (**Figure 2C**) based on all identified proteins showed a clear separation of samples in the different treatment groups. This

indicates that the generated data has a high resolution and could be used for evaluating treatment-specific protein profiles. Furthermore, unsupervised clustering resulted in two distinct clusters based on afatinib presence in the combination treatment.

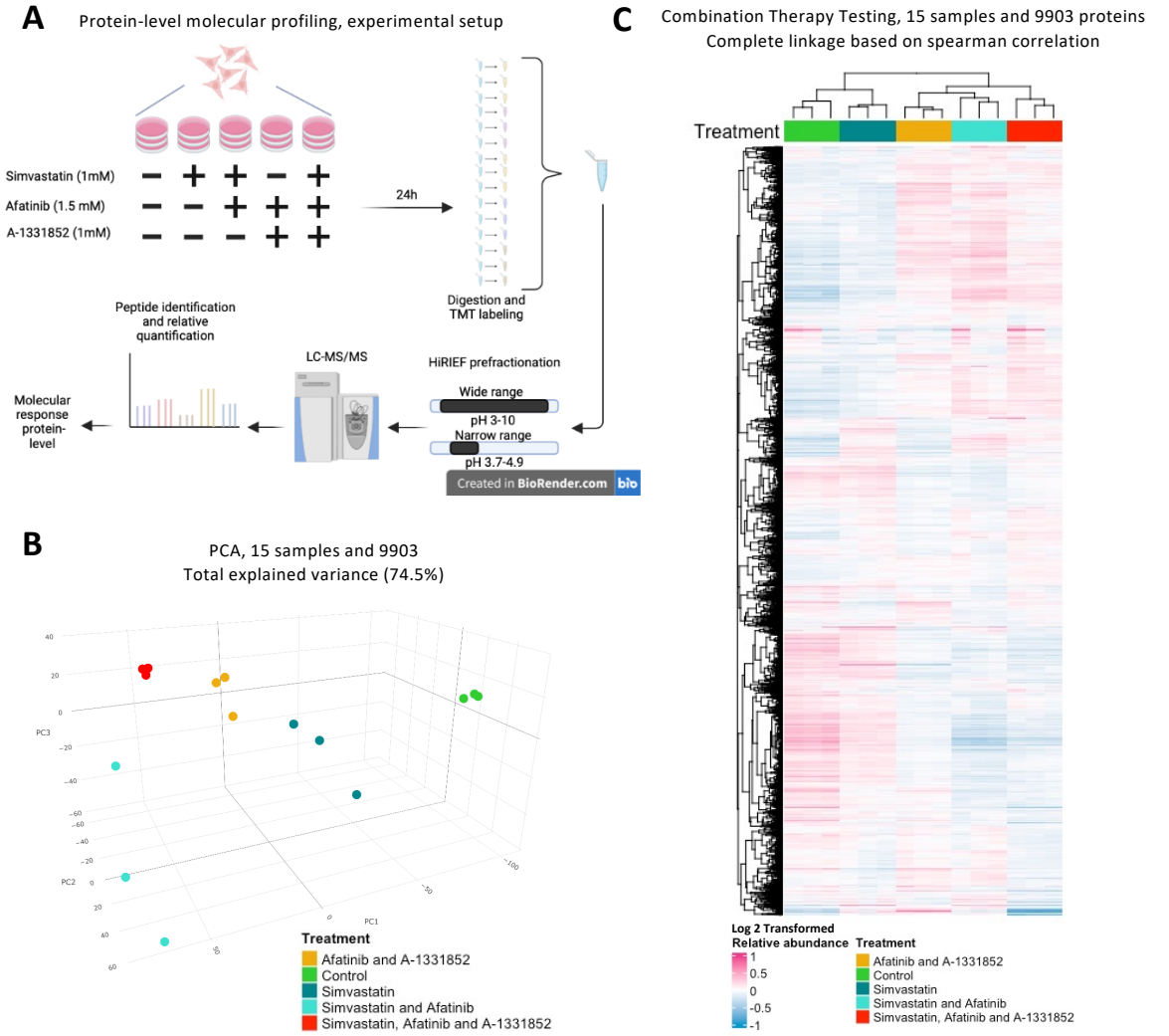

Figure 2. Molecular response profiling overview. **A**. Experimental setup for molecular profiling. Briefly, untreated cells (control) and cells treated with drugs in four different combinations for 24h in triplicate cell cultures were used in the experiment. In-depth protein-level analysis was then performed by using HiRIEF LC-MS with relative protein quantification between samples by TMT labelling. **B**. Principal-component analysis based on 9903 proteins that were identified and quantified by MS. **C**. Hierarchal clustering of 15 samples and 9903 proteins with spearman correlation-based distance and complete linkage.

Treatment-specific differential expression of proteins

Prior experiments performed in the group showed upregulation of senescence inducers CDKN1A (p21), CDKN1B (p27) and downregulation of the cell cycle regulator RB1 after afatinib treatment, indicating that EGFR-TKI treatment in these cells results in induction of senescence. When adding A-1331852 to the afatinib treatment, both the induction of CDKN1A and CDKN1B and the reduction of RB1 were hampered. Further, in the combination therapy treated samples, a decrease in TP53 was observed potentially explaining the reduced CDKN1A

and CDKN1B as TP53 is a known transcription factor for these genes. Further, an upregulation of several key proteins in the mevalonate pathway such as HMGCR, HMGCS1, APOB, DHCR24, MSMO1, SQLE, FDFT1 and LDLR was evident in the double combination-treated cells (**Figure 3a**). In the current experiment where the triple combination (simvastatin, afatinib and A-1331852) was compared to the afatinib and A-1331852 combination treatment, a significant upregulation of HMGCR was detected (**Figure 3b)**. This finding was expected since statins are known to trigger feedback upregulation of HMGCR through transcription activation of SREBP[21]. No significant difference in protein levels were detected for CDKN1A, CDKN1B and TP53 (**Figure 3b)**. Upon a comparison of the differentially expressed proteins in the different combinations (**Figure 3c,d**), the triple combination was found to have 17 and 76 uniquely upregulated and downregulated proteins, respectively. Interestingly, transcription factor JUND and its paralog JUN were found among the upregulated proteins which are both known to be important for cell cycle progression and EMT [36] . The downregulated proteins were to a large extent complement proteins such as C2, C8B, C6, C5, and C3 [37] or proteins involved in coagulation such as SERPINF2, SERPINA1, and SERPINA3 [38].

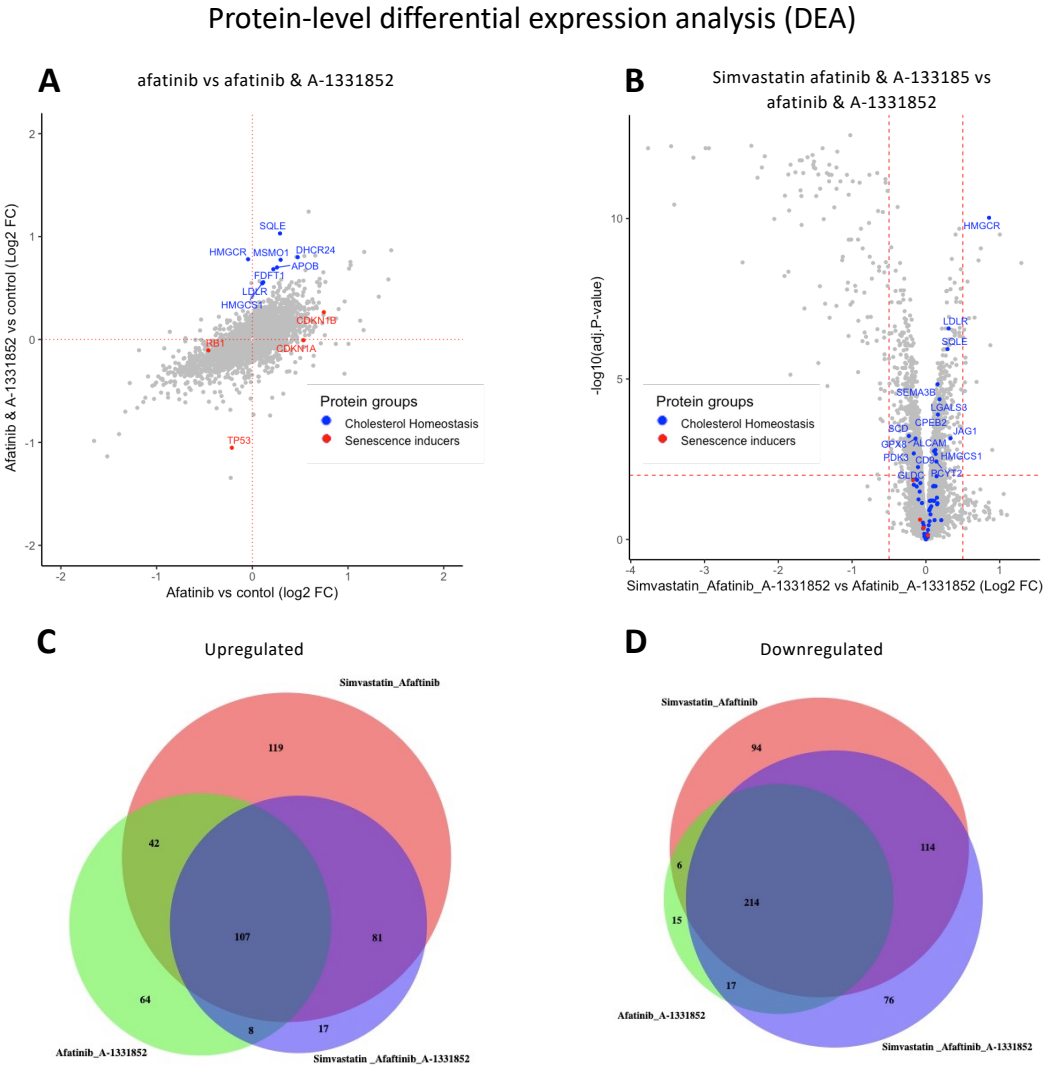

Figure 3. Protein level differential expression. A. Fold changes of afatinib-treated cells compared to fold changes of afatinib & A-1331852- treated cells. Data set filtered on adjusted P-value 0.01 for either afatinib treatment or afatinib & A-1331852 treatment. B. Volcano plot comparing simvastatin, afatinib and A-1331852 treatment with afatinib & A-1331852 treatment. C. Venn diagram of proteins with Fold change > 0.5 and adjusted P-value below 0.01.

Simvastatin affects cell cycle proliferation and cholesterol homeostasis in triple combination-based therapy

To see how groups of proteins which are representative of certain biological states or processes were altered when simvastatin was added to afatinib and A-1331852 combination, gene set enrichment analysis (GSEA) was performed. The analysis resulted in 10 and 9 significantly up- and down-regulated gene sets, respectively. Comparing the double combination with the triple combination showed that the addition of simvastatin resulted in significant upregulation of cholesterol synthesis pathway. This was an expected finding due to the feedback upregulation of proteins in cholesterol synthesis pathway that statins are known to trigger [19]. Interestingly, the epithelial-mesenchymal transition gene set was also significantly activated. This trans-

differentiation process has been linked both to sensitivity to statin treatment[39] and resistance to multiple targeted therapies [10]. Several gene sets related to proliferation were suppressed such as G2M checkpoint or E2F targets. This supports the hypothesis that the effect of the therapy is increased by the addition of simvastatin, see **Figure 4.**

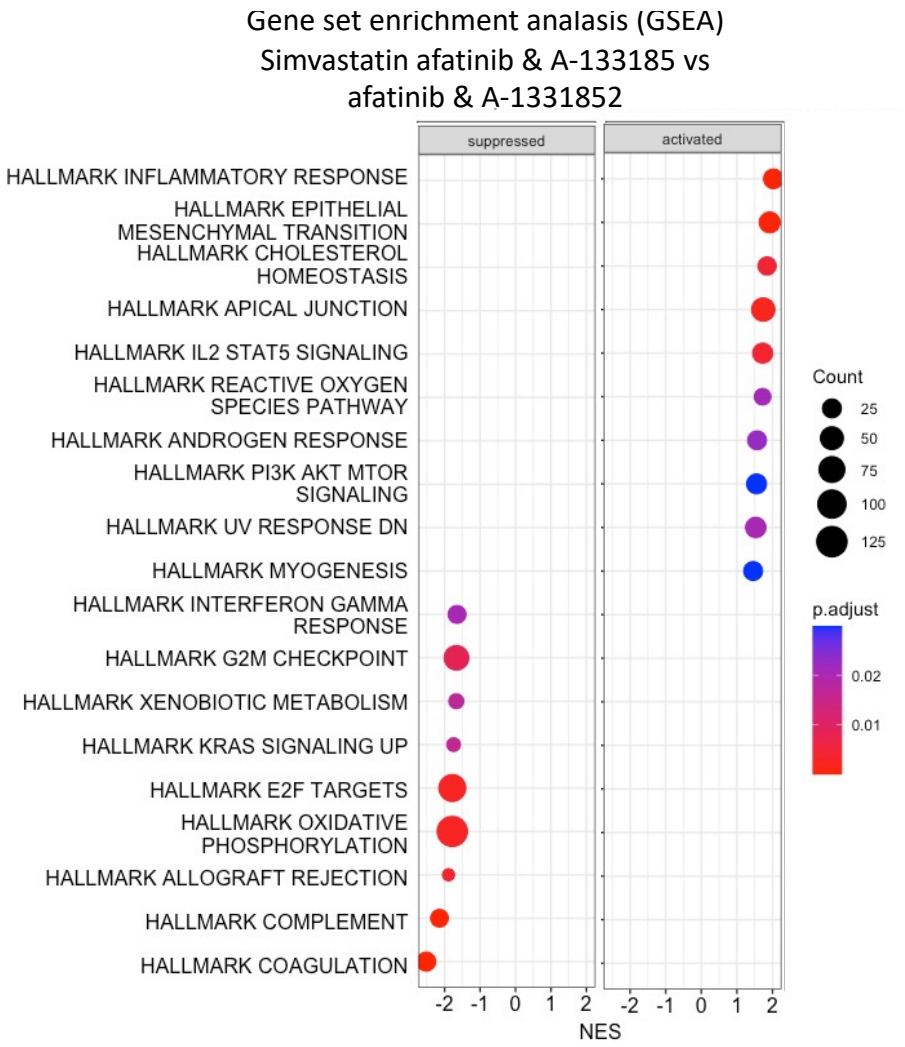

Figure 4. Comparing biological states and processes between cells treated with either simvastatin, afatinib and A-2331852 or afatinib and A-1331852. Gene set enrichment analysis performed with MSigDB Hallmarks datasets (50 gene sets) on a ranked list of fold changes comparing simvastatin, afatinib & A-1331852 treatment with afatinib & A-1331852 treatment showing gene sets with a FDR q-value below 0.05 plotted against the normalized enrichment score

Discussion

This study explored if CDKN2A-deleted, EGFRwt epithelial cells were dependent on cholesterol synthesis after afatinib and A-1331852 combination treatment, by adding simvastatin to the drug combination. Interestingly, the triple combination of drugs affected viability in a dose-dependent manner and also the proteome, especially proteins involved in the cell cycle, cholesterol homeostasis, and epithelial to mesenchymal transition. All those biological activities are strongly linked to adenocarcinoma pathology.

High-throughput DSRT was done on CDKN2A deleted, EGFRwt NCI-H292 cells to evaluate treatment-specific effects on viability between simvastatin, afatinib and A-1331852. Both simvastatin and A-1331852 monotherapies showed a limited impact on viability. In contrast, afatinib monotherapy showed a rapid dose-dependent drop in viability down to 40%, reached at a concentration of 10 nM. Further increased concentrations did not result in any significant decrease in viability which is expected since the drug is affecting proliferation [13]. Therefore, we believe that afatinib treatment in this model system is effectively setting cells in a non-proliferative state, corresponding to 40% viability compared to untreated control cells. Furthermore, drug response curves for all combination therapies have a similar impact on viability as afatinib monotherapy and the effects are probably driven by afatinib alone. Interestingly, we see that increasing the dose of afatinib to 1500 nM in the triple combination results in a decrease in viability compared to afatinib monotherapy and double combination treatments. This viability decreases down to 21% indicates induction of cell death because the viability readout is in between what we believe could be a threshold of a non-proliferative state (40%) and (0%) which corresponds to complete cell death. Furthermore, dose and treatment duration are important variables to consider when performing viability tests [22]. Going forward, it would be of interest to study how these variables interplay. More specifically, long-term assays such as a clonogenic assay should better reflect the actual survival of cells and the capacity for cell division which would increase our understanding of the combination therapy effects.

As mentioned, afatinib has an impact on the cell cycle and proliferation [13]. Prior experiments done in the group shows that afatinib treatment results in upregulation of CDKN1A and CDKN1B, both known to inhibit cells from going into S-phase and thereby inducing cell cycle arrest [40]. Both these cyclin dependent kinase inhibitors are also known to be inducers of TIS [15] which indicates that CDKN2A deleted EGFRwt epithelial cells might use senescence as an escape mechanism to afatinib treatment. However, it takes TIS at least 10 days to be fully activated, making it difficult to draw any conclusions. Therefore, long term experiments such as a clonogenic assay could be performed to study the development of TIS by stainings of senescence marker senescence-associated (SA-βgal) at multiple time points [41]. Alternatively, cell cycle inducement of senescence where CDKN2A together with RB1(transcriptionally regulated by P53) has been described [42]. Since CDKN2A is deleted in this cell line and no hyperactivation of P53 is detected in this setup cell cycle mediated inducement of senescence is unlikely to occur. Adding the senolytic compound A-1331852 to aftainib treatment has a normalizing effect on both CDKN1A and CDKN1B suggesting an explanation to the synergistic effects of these to drugs. Furthermore, CDKN2A is thought to have an role in maintaining senescence, meaning that cells harboring this deletion might not be able to maintain a senescent phenotype [43]. In addition, no significant alterations in protein levels of any of these senescence inducers could be observed by the addition of simvastatin to the triple

combination. GSEA analysis show significant suppression of both E2F target and G2M checkpoint gene-sets which could be an add-on effect of simvastatin since it is known to impact cell cycle and proliferation [44]. In contrast to this finding, we see significant upregulation of transcription factor JUN and its paralog JUND which both have been described to activate proliferation and drive EMT [36]. Potentially this could be a feed-back mechanism activated by the triple combination therapy as a primary resistance mechanism. However, levels of epithelial marker E-cadherin or mesenchymal cell marker vimentin were not significantly altered. Again, long term experiments would probably be necessary for validation of such trans-differentiation processes.

By performing protein-level molecular profiling we could investigate how cholesterol synthesis was altered by the addition of simvastatin to afatinib and A-1331852 combination treatment. GSEA analysis revealed significant upregulation of cholesterol homeostasis. Furthermore, differential expression analysis showed significant upregulation of HMGCR and indications of LDLR upregulation. Taken together, these findings strongly indicate that simvastatin successfully triggers feedback transcriptional activity of SREBP by binding to HMGCR. and thereby triggers feedback transcriptional activity of SREBP [21]. However, statin sensitivity has been inversely correlated with the cells ability to activate this feedback response; therefore, cancer cells with impaired feedback regulation are more sensitive to statin treatment [45]. Statin-mediated feedback of SREBP can also effectively be targeted with FDA-approved dipyridamole which thereby potentiates statin anti-cancer activity [46]. On the other hand, the GSEA analysis shows significant activation of the reactive oxygen species pathway which often correlates with the genes carrying the apoptosis hallmark cause of overlap in the gene sets [47]. In line with this finding, one mechanism of statin toxicity is deprivation of GGPP-derived CoQ which is identified by an increased level of reactive oxygen species (ROS) and apoptosis[25, 26]. However, we can't see any effects on the apoptosis hallmark in the GSEA analysis or detect any apoptotic markers such as BAX or BAK being upregulated. One possible explanation might be that the intracellular ROS has not yet induced apoptosis at the timepoint used for LC-MS (24h)[48]. Another explanation could be that antioxidants might blunt the ROS toxicity and, if that is the case, blocking of cysteine importer with xCT transporter-lowering MEK inhibitor has proved to potentiate statins' anti-cancer activity [26]. Cells of mesenchymal linage are known to be more sensitive to statin treatment [49]. However, the inducement of EMT has been reported to be correlated with sensitivity to statins [39]. The significant activation of EMT gene set in GSEA might thereby indicate that addition simvastatin might be effective in this setting.

Our results indicate that a triple combination of afatinib, A-1331852, and simvastatin has a synergistic effect in killing CDKN2A deleted EGFR wild-type epithelial cells. The concentrations of each drug could be decreased, probably leading to reduced adverse toxicity. However, for this combination treatment to be implemented in a clinical setting, subsequent steps are needed; The combination would need to be proven safe with maintained anti-cancer effects. Initially, in animal models, like xenograft mice, before being evaluated in clinical trials. The target population for such a trial would be patients with CDKN2A deletion and EGFRwt NSCLC adenocarcinoma. However, DNA deletions in general are difficult to detect with panel sequencing which is currently used for DNA mutation analysis in a clinical setting, which poses difficulties for using CDKN2A deletion as a predictive biomarker [50]. Simvastatin and afatinib are marketed drugs and have already been tested as a combination therapy for NSCLC in a phase II trial. Simvastatin has shown to be tolerated at much higher doses than what's usually prescribed [51] whereas Bcl-XL inhibitors have documented issues with dose dependent on-

target platelet toxicity [52]. Recent advancements in drug delivery could help to overcome this issue. To circumvent these unwanted effects specific proteolysis-targeting chimeras (PROTACs) have been developed, showing promising results [53]. To our knowledge A-1331852 has never been tested in human and A-1331852 would need to be tested with simvastatin and afatinib in a phase I dose escalation trial to evaluate an optimal triple combination.

This study has several strengths. The use of high sensitivity LC-MS technique, that can reach a great analytical depth [30]. Thereby, the technique enables profiling of molecular patterns linked to disease such as NSCLC. In addition, treatment specific protein level responses can be revealed and thereby also an understanding of immediate resistance mechanisms. In the future it would be of interest to test additional concentrations of the drug combinations used as well as longer exposures (such in a clonogenic assay) in order to find an optimal treatment effect. It would also be interesting to do metabolic measurements to see how successful the feedback mechanism of SREBP is to rescue cholesterol synthesis from simvastatin treatment. Only one cell line was used when the mevalonate pathway was found to be upregulated in response to afatinib and A-1331852 combination treatment. It is thereby difficult to know how generalisable this suggested triple combination treatment would be. More cell lines with CDKN2A deletion EGFRwt would have used for testing in order to gain such knowledge. Lastly, 2D cultures that were used in this experiment are known to generate very robust results [54]. It is important to point out that plastic dishes are a very stiff material for cell culturing and it does not mirror the natural microenvironment of the lung, which is an elastic tissue in constant movement affecting cells well-being and behavior [55].

To summarize, our results document that simvastatin synergizes with afatinb and A-1331852 combination treatment in CDKN2A deleted epithelial cells with wild type EGFR. However, these effects might be blunted by feedback upregulation of the mevalonate pathway through SREBP transcriptional activity. Long-term viability assays and metabolic assays would need to be performed in order to gain more knowledge on the effectiveness of the treatment and by which mode of action simvastatin is exhibiting anti-cancer effects.

Acknowledgments

Being a student at LTH has been an existing and eventful part of my life for which I am grateful. Therefore, I would like to start by thanking all my fellow students who have been sharing this journey with me and thereby making it so special.

I would also like to thank Professor **Janne Lehtiö** for letting me perform my master thesis in his group at the Karolinska Institutet and for connecting me with my supervisors. For them, I would like to start of by thanking **Lukas Orre** for letting me take part in this exciting project and for introducing me to the fields of molecular profiling and lung cancer as well as guiding me through this project. Next up, I would like to thank **Olena Berkovska** for providing me with lab protocols, guiding me in the cell lab and for being available to answer questions when needed. Then, I would like to thank **Yanbo Pan** for helping me with the experimental and computational work and for competitive tennis matches. Additionally, I would like to thank **Giorgos** for helping me with running the mass spec samples. I would also like to thank **Konstantin** not only for guiding me and Yanbo through the new version of the proteome discoverer but also for maintaining a robust fika culture in the group.

I would also like to take the opportunity to thank the whole group of the Lehtiö lab for enjoyable discussions at lunch breaks and thanks **Harris** for organizing activities with the other students such as going to the opera or the pub.

I would also like to take the opportunity to thank my supervisor at LTH **Sara Ek** for being available to answer questions about how the thesis should be conducted.

Finally, I would like to thank my family for all the support during these years, this master thesis is dedicated to them.

References

1. Ferlay, J., et al., *Cancer statistics for the year 2020: An overview.* Int J Cancer, 2021.
2. *State of Lung Cancer*, A.L. Assosiation, Editor. 2020.
3. Chen, R., et al., *Emerging therapeutic agents for advanced non-small cell lung cancer.* J Hematol Oncol, 2020. **13**(1): p. 58.
4. *Lung Cancer - Non-Small cell: Statistics*. 2022 2022-09-22]; Available from: https://www.cancer.net/cancer-types/lung-cancer-non-small-cell/statistics.
5. Zheng, M., *Classification and Pathology of Lung Cancer.* Surg Oncol Clin N Am, 2016. **25**(3): p. 447-68.
6. Lehtio, J., et al., *Proteogenomics of non-small cell lung cancer reveals molecular subtypes associated with specific therapeutic targets and immune evasion mechanisms.* Nat Cancer, 2021. **2**(11): p. 1224-1242.
7. Bashraheel, S.S., A. Domling, and S.K. Goda, *Update on targeted cancer therapies, single or in combination, and their fine tuning for precision medicine.* Biomed Pharmacother, 2020. **125**: p. 110009.
8. Vasan, N., J. Baselga, and D.M. Hyman, *A view on drug resistance in cancer.* Nature, 2019. **575**(7782): p. 299-309.
9. Zhou Tran, Y., et al., *Immediate Adaptation Analysis Implicates BCL6 as an EGFR-TKI Combination Therapy Target in NSCLC.* Mol Cell Proteomics, 2020. **19**(6): p. 928-943.
10. Song, K.A. and A.C. Faber, *Epithelial-to-mesenchymal transition and drug resistance: transitioning away from death.* J Thorac Dis, 2019. **11**(6): p. E82-e85.
11. Mok, T.S., et al., *Gefitinib or carboplatin-paclitaxel in pulmonary adenocarcinoma.* N Engl J Med, 2009. **361**(10): p. 947-57.
12. Sridhar, S., L. Seymour, and F. Shepherd, *Inhibitors of epidermal-growth-factor receptors: A review of clinical research with a focus on non-small-cell lung cancer.*Lancet Oncol, 2003. **4**: p. 397-406.
13. Garassino, M.C., et al., *Erlotinib versus docetaxel as second-line treatment of patients with advanced non-small-cell lung cancer and wild-type EGFR tumours (TAILOR): a randomised controlled trial.* Lancet Oncol, 2013. **14**(10): p. 981-8.
14. Li, R., et al., *Niclosamide overcomes acquired resistance to erlotinib through suppression of STAT3 in non-small cell lung cancer.* Mol Cancer Ther, 2013. **12**(10): p. 2200-12.
15. Campisi, J., *Aging, cellular senescence, and cancer.* Annu Rev Physiol, 2013. **75**: p. 685-705.
16. Clendening, J.W., et al., *Dysregulation of the mevalonate pathway promotes transformation.* Proc Natl Acad Sci U S A, 2010. **107**(34): p. 15051-6.
17. Duncan, R.E., A. El-Sohemy, and M.C. Archer, *Mevalonate promotes the growth of tumors derived from human cancer cells in vivo and stimulates proliferation in vitro with enhanced cyclin-dependent kinase-2 activity.* J Biol Chem, 2004. **279**(32): p. 33079-84.
18. Juarez, D. and D.A. Fruman, *Targeting the Mevalonate Pathway in Cancer.* Trends Cancer, 2021. **7**(6): p. 525-540.
19. Kirby, M.G., et al., *Prescription switching: Rationales and risks.* Int J Clin Pract, 2020. **74**(1): p. e13429.
20. Ward, N.C., G.F. Watts, and R.H. Eckel, *Statin Toxicity.* Circ Res, 2019. **124**(2): p. 328-350.
21. Brown, M.S. and J.L. Goldstein, *Lowering plasma cholesterol by raising LDL receptors.* N Engl J Med, 1981. **305**(9): p. 515-7.
22. Longo, J., et al., *Statins as Anticancer Agents in the Era of Precision Medicine.* Clin Cancer Res, 2020. **26**(22): p. 5791-5800.
23. Jiao, Z., et al., *Statin-induced GGPP depletion blocks macropinocytosis and starves cells with oncogenic defects.* Proc Natl Acad Sci U S A, 2020. **117**(8): p. 4158-4168.

24. Wang, M. and P.J. Casey, *Protein prenylation: unique fats make their mark on biology.* Nat Rev Mol Cell Biol, 2016. **17**(2): p. 110-22.
25. Kaymak, I., et al., *Mevalonate Pathway Provides Ubiquinone to Maintain Pyrimidine Synthesis and Survival in p53-Deficient Cancer Cells Exposed to Metabolic Stress.* Cancer Res, 2020. **80**(2): p. 189-203.
26. McGregor, G.H., et al., *Targeting the Metabolic Response to Statin-Mediated Oxidative Stress Produces a Synergistic Antitumor Response.* Cancer Res, 2020. **80**(2): p. 175-188.
27. Han, J.Y., et al., *A randomized phase II study of gefitinib plus simvastatin versus gefitinib alone in previously treated patients with advanced non-small cell lung cancer.* Clin Cancer Res, 2011. **17**(6): p. 1553-60.
28. Lee, J.S., et al., *Statins enhance efficacy of venetoclax in blood cancers.* Sci Transl Med, 2018. **10**(445).
29. Hughes, C.S., et al., *Single-pot, solid-phase-enhanced sample preparation for proteomics experiments.* Nat Protoc, 2019. **14**(1): p. 68-85.
30. Branca, R.M., et al., *HiRIEF LC-MS enables deep proteome coverage and unbiased proteogenomics.* Nat Methods, 2014. **11**(1): p. 59-62.
31. Potdar, S., et al., *Breeze: an integrated quality control and data analysis application for high-throughput drug screening.* Bioinformatics, 2020. **36**(11): p. 3602-3604.
32. W. N. Venables, B.D.R., *Modern Applied Statistics with S*. Statistics and Computing. 2002: Springer New York, NY.
33. Gu, Z., R. Eils, and M. Schlesner, *Complex heatmaps reveal patterns and correlations in multidimensional genomic data.* Bioinformatics, 2016. **32**(18): p. 2847-9.
34. Zhu, Y., et al., *DEqMS: A Method for Accurate Variance Estimation in Differential Protein Expression Analysis.* Mol Cell Proteomics, 2020. **19**(6): p. 1047-1057.
35. Wu, T., et al., *clusterProfiler 4.0: A universal enrichment tool for interpreting omics data.* Innovation (Camb), 2021. **2**(3): p. 100141.
36. Meixner, A., et al., *Jun and JunD-dependent functions in cell proliferation and stress response.* Cell Death Differ, 2010. **17**(9): p. 1409-19.
37. Janeway CA Jr, T.P., Walport M, et al, *Immunobiology*. Vol. 5. 2001, New York.
38. Bao, J., et al., *Serpin functions in host-pathogen interactions.* PeerJ, 2018. **6**: p. e4557.
39. Yu, R., et al., *Statin-Induced Cancer Cell Death Can Be Mechanistically Uncoupled from Prenylation of RAS Family Proteins.* Cancer Res, 2018. **78**(5): p. 1347-1357.
40. Abukhdeir, A.M. and B.H. Park, *P21 and p27: roles in carcinogenesis and drug resistance.* Expert Rev Mol Med, 2008. **10**: p. e19.
41. Debacq-Chainiaux, F., et al., *Protocols to detect senescence-associated beta-galactosidase (SA-betagal) activity, a biomarker of senescent cells in culture and in vivo.* Nat Protoc, 2009. **4**(12): p. 1798-806.
42. Serrano, M., et al., *Oncogenic ras provokes premature cell senescence associated with accumulation of p53 and p16INK4a.* Cell, 1997. **88**(5): p. 593-602.
43. Robles, S.J. and G.R. Adami, *Agents that cause DNA double strand breaks lead to p16INK4a enrichment and the premature senescence of normal fibroblasts.* Oncogene, 1998. **16**(9): p. 1113-23.
44. Liang, Y.W., et al., *Preclinical Activity of Simvastatin Induces Cell Cycle Arrest in G1 via Blockade of Cyclin D-Cdk4 Expression in Non-Small Cell Lung Cancer (NSCLC).* Int J Mol Sci, 2013. **14**(3): p. 5806-16.
45. Clendening, J.W., et al., *Exploiting the mevalonate pathway to distinguish statin-sensitive multiple myeloma.* Blood, 2010. **115**(23): p. 4787-97.
46. Pandyra, A., et al., *Immediate utility of two approved agents to target both the metabolic mevalonate pathway and its restorative feedback loop.* Cancer Res, 2014. **74**(17): p. 4772-82.
47. Liberzon, A., et al., *The Molecular Signatures Database (MSigDB) hallmark gene set collection.* Cell Syst, 2015. **1**(6): p. 417-425.

48. Redza-Dutordoir, M. and D.A. Averill-Bates, *Activation of apoptosis signalling pathways by reactive oxygen species.* Biochim Biophys Acta, 2016. **1863**(12): p. 2977-2992.
49. Warita, K., et al., *Statin-induced mevalonate pathway inhibition attenuates the growth of mesenchymal-like cancer cells that lack functional E-cadherin mediated cell cohesion.* Sci Rep, 2014. **4**: p. 7593.
50. Austin-Tse, C.A., et al., *Best practices for the interpretation and reporting of clinical whole genome sequencing.* NPJ Genom Med, 2022. **7**(1): p. 27.
51. van der Spek, E., et al., *Dose-finding study of high-dose simvastatin combined with standard chemotherapy in patients with relapsed or refractory myeloma or lymphoma.* Haematologica, 2006. **91**(4): p. 542-5.
52. Negi, A. and A.S. Voisin-Chiret, *Strategies to Reduce the On-Target Platelet Toxicity of Bcl-x(L) Inhibitors: PROTACs, SNIPERs and Prodrug-Based Approaches.* Chembiochem, 2022. **23**(12): p. e202100689.
53. Pal, P., et al., *Discovery of a Novel BCL-X(L) PROTAC Degrader with Enhanced BCL-2 Inhibition.* J Med Chem, 2021. **64**(19): p. 14230-14246.
54. Jensen, C. and Y. Teng, *Is It Time to Start Transitioning From 2D to 3D Cell Culture?* Front Mol Biosci, 2020. **7**: p. 33.
55. Rosmark, O., et al., *A tunable physiomimetic stretch system evaluated with precision cut lung slices and recellularized human lung scaffolds.* Front Bioeng Biotechnol, 2022. **10**: p. 995460.